Characterization of Purine-Motif Triplex DNA-Binding Proteins in HeLa Extracts†

Marco Musso,‡ Laura D. Nelson, and Michael W. Van Dyke*

Department of Tumor Biology, The University of Texas M. D. Anderson Cancer Center, Houston, Texas 77030

Received July 17, 1997; Revised Manuscript Received December 18, 1997

ABSTRACT: One piece of evidence indicating that triple-helical DNAs exist in vivo would be the demonstration of cellular proteins that recognize such structures. Using oligonucleotide probes containing a GT-rich purine-motif triplex, proteins from either HeLa nuclear or cytoplasmic extracts and electrophoretic mobility shift assays, we identified four specific human protein−triplex complexes. Proteins in these complexes did not recognize an analogous homopurine/homopyrimidine duplex DNA or a pyrimidine-motif triplex but did recognize purine-motif triplexes regardless of whether they possessed a phosphodiester or phosphorothioate backbone in the third strand or involved A*AT instead of T*AT base triplets. For each of these proteins, binding affinity increased with increasing triplex length. For some triplex-binding proteins, a weak affinity was noted for individual G-rich oligonucleotides, though this may actually reflect an affinity for quadruplex structures, which these oligonucleotides are prone to adopt. Ion exchange chromatographic fractionation of HeLa nuclear extracts indicated that at least three different proteins were responsible for the observed electrophoretic mobility shifts. Southwestern blotting methods identified three major polypeptides, with apparent molecular masses of 100, 60, and 15 kDa, that preferentially recognized purine-motif triplexes. These data demonstrate the existence of eukaryotic proteins that specifically recognize one triplex motif and support the idea of a biological role for triple helical DNA.

It has long been recognized that certain DNA sequences can preferentially adopt a triple-helical, or triplex, structure under the proper conditions (*1*). Originally investigated with homopolymers and more recently with oligonucleotides, two types, or motifs, of triplexes have been characterized (reviewed in 2). Both involve recognition of homopurine/homopyrimidine stretches of duplex DNA by a third strand residing in the duplex major groove, with hydrogen bonding occurring especially through the N-7 position of the purines within the duplex. In the pyrimidine motif (Py-motif),[1] the third strand is pyrimidine-rich and is parallel to the homopurine strand of the duplex. Base triplets in this motif include C^+*GC and T*AT, with Hoogsteen hydrogen bonding occurring between the third base and the purine within the Watson−Crick base pair. Under physiological conditions that do not favor protonation of cytosine, the preferred Py-motif third strand is T-rich. In the purine motif (Pu-motif), the third strand is purine-rich, antiparallel to the homopurine strand of the duplex, and interacts through reverse Hoogsteen hydrogen bonding. Base triplets include A*AT and G*GC, though T*AT triplets are also observed and in some cases are more stable than corresponding A*AT triplets (*3*, *4*). Under most conditions the G*GC triplet exhibits the greatest stability, and thus the preferred purine-motif third strand is typically G-rich.

Most studies have focused on intermolecular triplexes, where the third strand is a separate molecule from the duplex. However, given suitable sequence and environmental conditions, intramolecular triplexes can also be formed (*5*). For these, conditions such as a high degree of torsional stress promote dissociation of part of a DNA duplex, thereby yielding two single-stranded regions, one of which interacts with a homopurine/homopyrimidine stretch on the remaining duplex to form an intramolecular triplex (reviewed in 6). Two motifs of intramolecular triplex have been identified, H-DNA and *H-DNA. These differ by the composition of the third strand, predominantly pyrimidine- or purine-rich, respectively, and correspond to the Py- and Pu-motifs described for intermolecular triplexes. As with their intermolecular counterparts, the rules governing intramolecular triplex formation (e.g., preferred base triplets, strand orientation) still apply. Thus under physiological conditions, either T-rich H-DNA or G-rich *H-DNA might be expected to predominate.

Several lines of evidence suggest that triplexes exist in eukaryotic cells and can influence different cellular processes, including transcription, replication, and recombination (*7*−*10*). However, direct proof for their existence in vivo remains lacking. If triplexes did exist in vivo, it is quite likely that cellular proteins that recognize such structures also exist. In the cases of several sequences thought to form H-DNA, those proteins found to recognize these sequences invariably bound either the single-stranded loop or the intact duplex (*11*−*14*). Presently, only two reports exist concerning

† This work was supported, in part, by research grants RPG-97-028-01-DHP from the American Cancer Society and G-1199 from the Welch Foundation and by a Physicians' Referral Service Award.

* Please address correspondence to this author at the Department of Tumor Biology (Box 79), University of Texas M. D. Anderson Cancer Center, 1515 Holcombe Boulevard, Houston, TX 77030. Tel.: (713) 792-8954. Fax: (713) 794-4784. E-mail: mishko@odin.mdacc.tmc.edu.

‡ Present address: Department of Biology and Genetics, University of Genoa, 16132 Genoa, Italy.

[1] Abbreviations: 3BP, triplex-binding protein; bt, base triplet; DE, DEAE-cellulose; EMSA, electrophoretic mobility shift assay; NE, nuclear extract; PC, phosphocellulose; Pu, purine; Py, pyrimidine; R_f, relative electrophoretic mobility; S100, cytoplasmic extract; TFO, triplex-forming oligonucleotide.

S0006-2960(97)01748-0 CCC: $15.00
Published on Web 02/10/1998

Table 1: Oligonucleotides

name	Sequence (5′ → 3′)
Triplex-forming oligonucleotides, purine motif	
ODN 1	TGGGTGGGGTGGGGTGGGT
Δ1-4	TGGGGTGGGGTGGGT
Δ1-5	GGGGTGGGGTGGGT
Δ1-7	GGTGGGGTGGGT
OPS[a]	tgggtggggtggggtgggt
PODN 1[b]	P~TGGGTGGGGTGGGGTGGGT
ODN 2	AGGGAGGGGAGGGGAGGGA
Triplex-forming oligonucleotides, pyrimidine motif	
PODN 3	P~TTTCTTTTTCTTTTTTT
Duplex probe oligonucleotides, purine motif	
Pu-CT	AGCTATCCCTCCCCTCCCCTCCCTTAGGA
Pu-GA	AGCTTCCTAAGGGAGGGGAGGGGAGGGAT
Duplex probe oligonucleotides, pyrimidine motif	
Py-AG	GTGCAGATCTAAAGAAAAAGAAAAAAA
Py-TC	AGCTTTTTTTCTTTTTCTTTAGATCTGCACTGCA

[a] Nucleotides not capitalized refer to phosphorothioate linkages. [b] P~ refers to a psoralen−hexyl moiety.

identification of cellular triplex-binding proteins, in both cases reporting a 55-kDa human (HeLa) protein that recognizes pyrimidine-motif triplexes (*15*, *16*).

Using electrophoretic mobility shift assays (EMSA), we report here several HeLa proteins that specifically recognize Pu-triplexes. These proteins do not recognize Py-triplexes or double-stranded DNAs, but some have a weak affinity for single-stranded DNAs capable of G-quartet formation. Initial chromatography indicates at least three Pu-triplex-binding proteins (Pu-3BPs) are present in HeLa cell extracts. Using Southwestern blotting methods, several HeLa proteins were found to specifically bind Pu-triplexes. The cellular roles of these proteins and their implications regarding the utility of triplexes as gene therapeutics are discussed.

MATERIALS AND METHODS

Oligonucleotides and DNA Probes. Sequences of triplex-forming oligodeoxyribonucleotides (TFOs) and oligodeoxyribonucleotides used to construct duplex targets for triplex formation are presented in Table 1. Psoralenated oligonucleotides, indicated by a "P" prefix in their name or by a "P~" appended to their sequence, contained a 4′-(hydroxymethyl)-4,5′,8-trimethylpsoralen−hexyl (Glen Research) moiety attached to their 5′ termini. The oligonucleotide containing a phosphorothioate backbone (i.e., OPS) is identified by its sequence in lower case letters. All oligonucleotides were purified by *n*-butanol precipitation (*17*); however, those used in constructing duplex and triplex probes were also further purified by denaturing gel electrophoresis.

Duplex probes and competitor DNAs were made by annealing equimolar concentrations of complementary oligonucleotides at room temperature, followed by 3′ end-filling with Klenow and deoxyribonucleotides. In the case of

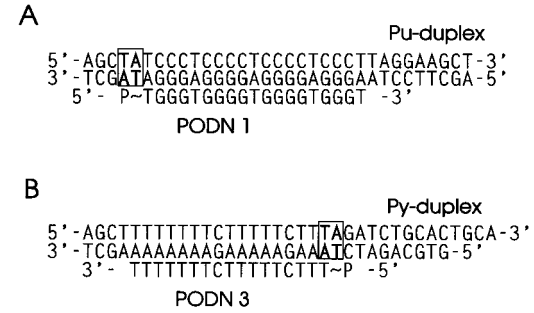

FIGURE 1: Schematic representations of the triplex probes used in characterizing 3BPs by EMSA. (A) Purine-motif triplex probe (Pu-triplex) composed of the Pu-duplex and the TFO PODN 1. P~, a psoralen−hexyl moiety covalently attached to the 5′ end of the oligonucleotide. The psoralen cross-linking site (5′-TA-3′) is boxed. (B) Pyrimidine-motif triplex probe (Py-triplex) composed of the Py-duplex and the TFO PODN 3.

labeled probes, [α-^{32}P]dATP was included in the reaction mixtures. Structures of these DNAs are shown in Figure 1. To form Pu-motif triplexes, Pu-duplex and a 10-fold molar excess of TFO were incubated for 60 min at 30 °C in a reaction mixture containing 40 mM Tris-HCl (pH 8.0), 100 mM $MgCl_2$, and 0.01% Nonidet P-40 (*18*). For Py-motif triplex formation, the corresponding Py-duplex, TFO PODN 3, and a buffer composed of 25 mM Tris-HCl (pH 6.0), 20 mM $MgCl_2$, and 70 mM NaCl were used instead. Structures of representative Pu- and Py-triplexes are shown in Figure 1. Psoralenated TFOs were covalently attached to the duplex DNA following triplex formation by irradiation at 365 nm for 10 min with a 6 W hand-held UV lamp. Under these circumstances, greater than 90% of the probe is present as photocross-linked triplexes (*19*).

HeLa Extracts and Chromatographic Fraction Preparation. Both nuclear (NE) and cytoplasmic (S100) extracts were prepared from exponentially growing HeLa (Attardi) cells using a modified Dignam protocol, essentially as previously described (*20*). Chromatographic fractions derived from HeLa NE were prepared by step elutions from phosphocellulose (P-11, Whatman) and DEAE-cellulose (DE-52, Whatman) columns, following established protocols (*21*). All fractions investigated had been exhaustively dialyzed against 20 mM Tris-HCl (pH 7.3), 100 mM KCl, 20% glycerol, 0.2 mM EDTA, 10 mM 2-mercaptoethanol, and 1 mM PMSF.

Electrophoretic Mobility Shift Assays (EMSA). To effect triplex binding by triplex-binding proteins (3BPs), protein mixtures were incubated for 20 min at 24 °C in a 10-μL volume containing buffer A (25 mM HEPES-Na^+ (pH 7.9), 50 mM KCl, 10% glycerol, 0.5 mM dithiothreitol), 1 mM $MgCl_2$, 1 nM probe DNA, 2 μg of poly(dI-dC) carrier DNA and additional competitor nucleic acids as indicated. Protein−probe complexes were then resolved by nondenaturing PAGE at 10 V/cm for 75 min through a 5% acrylamide/0.13% bisacrylamide gel containing 22 mM Tris-borate, 0.5 mM EDTA. To investigate triplex formation by various TFOs, we performed nondenaturing PAGE at 10 V/cm for 3 h through a 6% acrylamide/0.16% bisacrylamide gel containing 45 mM Tris-borate and 2 mM $MgCl_2$. In each case the probe-containing species were visualized by autoradiography and quantitated by densitometry.

Southwestern Blotting. Proteins mixtures were first resolved by SDS−PAGE using a 10% polyacrylamide gel and

then electroblotted at 55 V and 4 °C for 12 h onto nitrocellulose filters. Filters were washed six times for 5 min each with buffer A, blocked with 5% dried milk in buffer A for 90 min, washed with 0.25% dried milk in buffer A for 30 min, and then probed for 180 min with either a Klenow end-labeled photocross-linked PODN 1 Pu-triplex or the corresponding Pu-duplex (3000 cpm, at least 2 pM final) in 15 mL of buffer A, 2 mM $MgCl_2$, 0.125% milk, 0.05% Triton X-100, and 10 μg/mL poly(dI-dC). Probed filters were finally washed four times for 10 min each with buffer A and 2 mM $MgCl_2$. All filter manipulations were performed at 4 °C with continuous gentle agitation. The electrophoretic mobilities of triplex-binding proteins were visualized by autoradiography, and their apparent molecular weights were determined through comparison of blotted marker proteins stained with Fast Green FCF.

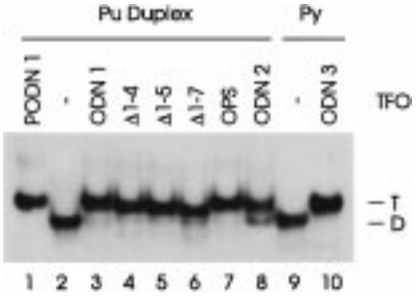

FIGURE 2: Triplex formation by TFOs. The abilities of different oligonucleotides to form either Pu- or Py-motif triplexes was investigated by EMSA using a nondenaturing polyacrylamide gel containing 2 mM Mg^{2+}. Reaction mixtures contained 1 nM of either the Pu-duplex or the Py-duplex and 10 nM of the TFO indicated. The relative mobilities of triplex (T) and duplex (D) probes are indicated at right.

RESULTS

Triplex Formation. To investigate proteins that bind purine-motif triplex DNA (3BPs), we chose as our probe a 19-base triplet (bt) triplex based on the TFO sequence 5′-TGGGTGGGGTGGGGTGGGT-3′, which demonstrates strong, sequence-specific binding in an antiparallel fashion to a G-rich homopurine, duplex DNA target (*3, 22*). A schematic representation of our standard triplex probe and the TFO and duplex DNA that compose it is shown in Figure 1A. Additional purine-motif triplexes based on the identical duplex target sequence but containing different TFOs were also investigated. A complete list of the TFOs used is provided in Table 1. These TFOs allowed us to investigate the effects of triplex length (12−19 bt) and base (GA- or GT-rich) and backbone composition (phosphodiester or phosphorothioate) on 3BP-binding specificity. To explore the triplex-motif specificity of 3BPs, a model 17-bt pyrimidine-motif triplex based on the TFO 5′-TTTCTTTTTCT-TTTTTT-3′ was also constructed (Figure 1B). Under near-physiological conditions, this TFO demonstrated strong, sequence-specific binding in a parallel fashion to an A-rich homopurine duplex DNA target (*23*). Note that the TFOs PODN 1 and PODN 3 contained a psoralen moiety covalently attached through a hexyl linker to their 5′ ends. These allowed the photocross-linking of the TFO to a 5-TA-3′ sequence (boxed in figure) adjacent to the triplex site within the duplex probe following triplex formation, resulting in a covalently bound triplex species that remained intact even under conditions that normally promote triplex dissociation (*19*).

Observation of possible protein−triplex binding requires that the triplexes investigated are efficiently formed and remain stable under binding conditions. This we had previously shown for triplexes containing the G-rich TFOs present in Table 1 (*18, 19, 24, 25*). To confirm these findings and demonstrate, in our hands, the stability of the Py-motif triplex used in this study, an EMSA analysis was performed. Pu- or Py-motif triplexes were formed under standard conditions (see Materials and Methods) and then resolved from their corresponding labeled duplex probes following electrophoresis through a nondenaturing 8% polyacrylamide gel containing 45 mM Tris-borate and 2 mM $MgCl_2$. Note, Mg^{2+} is required to maintain triplex integrity during electrophoresis (*18*). Psoralen-containing TFOs were photocross-linked to their duplex probes following triplex formation but prior to electrophoresis, as described above (*19*). As shown in Figure 2, most all of these TFOs demonstrated nearly complete triplex formation (greater than 95%), with the relative electrophoretic mobility of their triplex species consistent with TFO length. TFOs ODN 2 and Δ1-7 demonstrated slightly reduced levels of triplex species (77% and 90%, respectively). With ODN 2, this is consistent with previous affinity cleaving and DNase I footprinting studies that had demonstrated reduced purine-motif triplex formation with GA- versus GT-rich TFOs (*3, 22, 24*). With Δ1-7, this observation contrasts with DNase I footprinting and REPSA combinatorial studies demonstrating an optimal 12-mer G-rich TFO length (*25, 26*) and suggests that shorter triplexes may actually possess reduced stability during electrophoresis.

Interactions of HeLa Proteins with Pu-Motif Triplexes. To determine whether there are proteins in human cells that specifically recognize Pu-motif triplex DNA, an EMSA was performed. Human proteins (3 μg) from a Dignam-style HeLa NE were incubated for 20 min at room temperature in a 10-μL volume containing 25 mM HEPES−Na^+ (pH 7.9), 50 mM KCl, 10% glycerol, 0.5 mM dithiothreitol, 1 mM $MgCl_2$, and 2 μg of poly(dI-dC) carrier DNA, together with 1 nM radiolabeled DNA as either a covalently bound Pu-triplex (containing PODN 1), a noncovalently bound Pu-triplex (containing ODN 1), or the parent Pu-duplex DNA. The resulting complexes were then resolved by nondenaturing PAGE (5% acrylamide/0.13% bisacrylamide gel containing 22 mM Tris-borate and 0.5 mM EDTA) and visualized by autoradiography. From our preliminary studies, we found that optimal results were obtained when electrophoresis was performed without Mg^{2+} in the running buffer, presumably because protein−triplex complexes exhibit reduced stability under these conditions (M. Musso, unpublished observations). As shown in Figure 3, in the presence of HeLa NE several new, slower mobility species (H) were observed when a Pu-triplex probe was present but not when a corresponding duplex DNA probe was present. This result showed that Pu-motif 3BPs were present in HeLa NE. Protein binding occurred with both covalent and noncovalent triplex probes (lanes 2 and 4). This indicated that the binding was specific for the triplex and not for the psoralen moiety or the photocross-link. Similarly we observed no specific protein binding to a Pu-duplex probe containing only a positioned psoralen cross-link (data not shown). Data from the experiment in Figure 3 also provided an independent

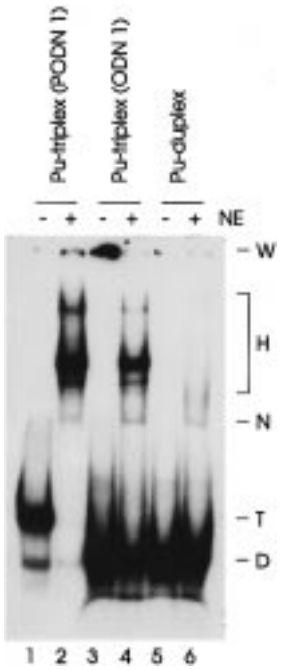

FIGURE 3: 3BP binding to covalently and noncovalently attached Pu-triplexes. EMSAs were performed on reaction mixtures containing 1 nM labeled probe, either the covalently bound Pu-triplex containing PODN 1 (lanes 1 and 2), the noncovalently bound Pu-triplex containing ODN 1 (lanes 3 and 4), or the Pu-duplex alone (lanes 5 and 6). Minus and plus refer to the absence and presence of 3 μg of HeLa NE in the reaction mixtures, respectively. Locations of the gel well (W), shifted species containing HeLa proteins (H), a nonspecific band (N), unbound triplex (T), and duplex (D) probes are indicated at right.

measure of cross-linking efficiency for the PODN 1 triplex probe. Given that a noncovalently bound Pu-motif triplex is unstable under these electrophoresis conditions, the amount of labeled probe remaining in a triplex species following electrophoresis would be indicative of the percentage of cross-linked TFO present (greater than 95%, compare lanes 1 and 3).

To better characterize the nature of the interactions between these putative 3BPs and DNA, competition experiments were performed. Note, unlike the aforementioned binding experiments with different labeled probes, competition experiments compare binding affinities for different DNAs under solution conditions and are not sensitive to differences in protein−DNA complex stabilities during electrophoresis. For these, binding reactions containing 1 nM radiolabeled PODN 1-triplex probe also contained 5−100 nM concentrations of unlabeled competitor DNAs, including either a covalently bound Pu-triplex (with PODN 1), a noncovalently bound Pu-triplex (with ODN 1), or the parent duplex itself. As shown in Figure 4A, four major complexes were observed when HeLa NE was present (lane 2), these having relative electrophoretic mobilities of 0.16, 0.20, 0.40, and 0.47 for the complexes H1, H2, H3, and H4, respectively. Relative abundances of these species were 5.8%, 13%, 55%, and 12% of the total label shifted. Identical mobility species were observed with HeLa S100 (Figure 4B), though their relative abundances were instead 3.9%, 16%, 22%, and 35%. With either NE or S100, all shifted species were effectively competed and free triplex probe recovered when increasing concentrations of either covalent or noncovalently bound cold triplex DNA was present (lanes 3−6 and 7−10). However,

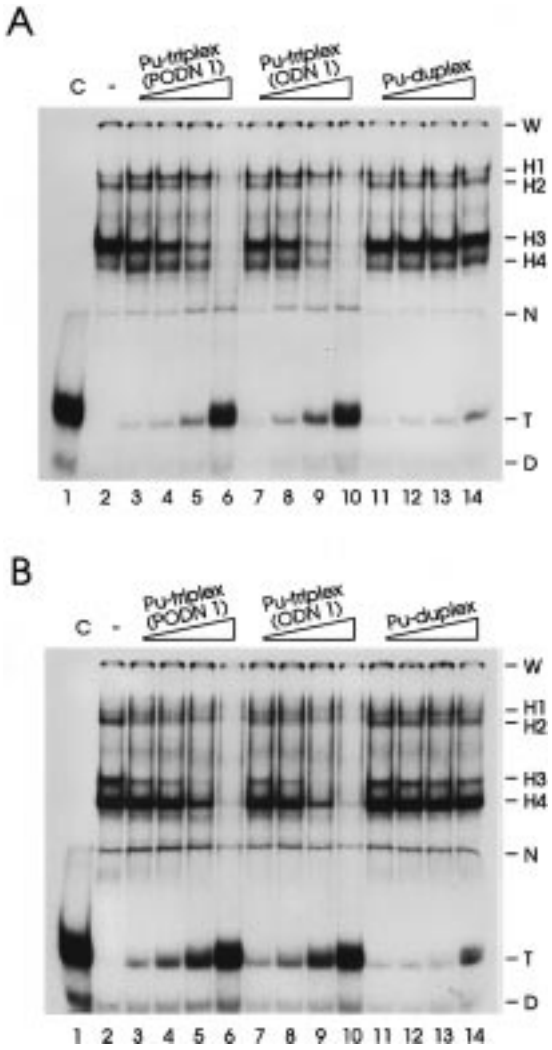

FIGURE 4: 3BPs in HeLa extracts. EMSAs were performed on reaction mixtures containing 1 nM labeled Pu-triplex (composed of the TFO PODN 1 covalently attached to the Pu-duplex), 3 μg of HeLa proteins, and increasing concentrations (either 5, 10, 25, or 100 nM) of competitor DNAs as indicated above each lane. Competitor DNAs included a covalently bound Pu-triplex (lanes 3−6), a noncovalently bound Pu-triplex (lanes 7−10), and the Pu-duplex (lanes 11−14). Control reactions performed either in the absence of added HeLa proteins (C, lane 1) or in the absence of competitor DNA (−, lane 2) are indicated above. (A) Binding reactions containing HeLa NE. Relative mobilities of different probe-containing species are indicated at right. (B) Binding reactions containing HeLa S100.

increasing concentrations (to 100 nM) of duplex competitor had no effect, suggesting that these species contained bona fide human 3BPs. Note that not all species were competed with equal efficiency. For example, with NE formation of the H3 complex was inhibited 50% when 6 nM triplex was present, while formation of the H1 complex was only inhibited 5% when 26 nM triplex was present. These differences could reflect the relative abundances and affinities of their corresponding 3BPs.

Binding Specificity of HeLa 3BPs. To further characterize the binding specificity of human 3BPs, a series of EMSA experiments using different competitor DNAs was undertaken. For example, to investigate the triplex structural features (e.g., base triplets, backbone composition) recognized by these proteins, competition assays with different types of triplexes were performed. Triplexes investigated

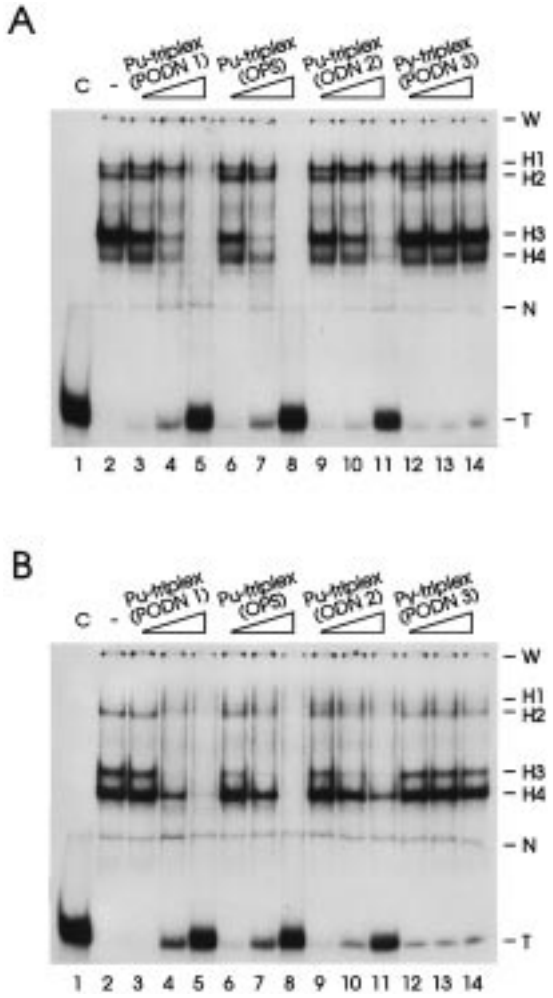

FIGURE 5: Triplex specificities of HeLa 3BPs. EMSAs were performed on reaction mixtures containing 1 nM labeled Pu-triplex (PODN 1), 3 μg of HeLa extract, and increasing concentrations (either 5, 25, or 100 nM) of competitor triplexes as indicated above each lane. Competitors included a covalently bound Pu-triplex (lanes 3−5), a noncovalently bound Pu-triplex containing the phosphorothioate TFO OPS (lanes 6−8), a noncovalently bound triplex containing the GA-rich TFO ODN 2 (lanes 9−11), and a covalently bound Py-motif triplex (lanes 12−14). (A) HeLa NE. (B) HeLa S100.

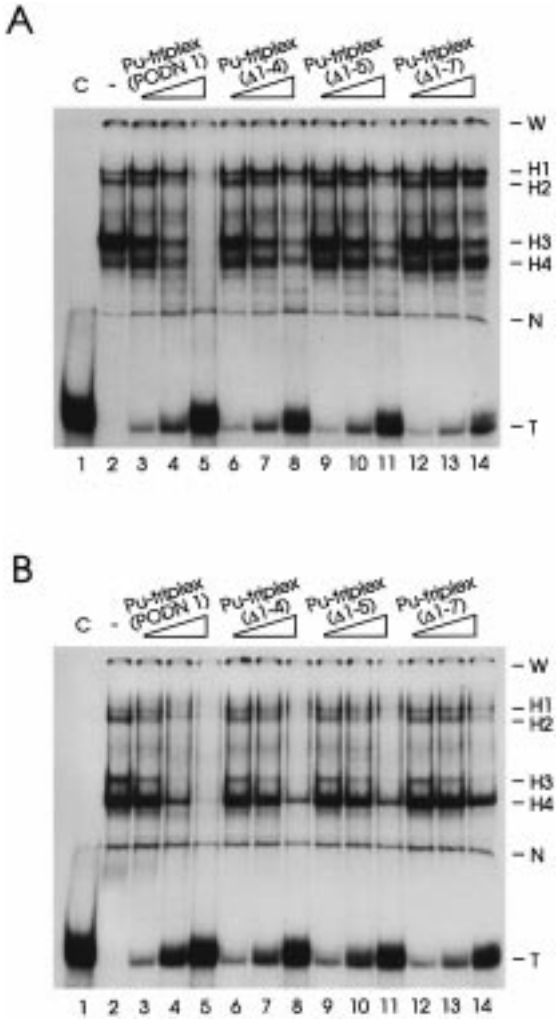

FIGURE 6: 3BP binding to different length Pu-triplexes. EMSAs were performed on reaction mixtures containing 1 nM labeled Pu-triplex (PODN 1), 3 μg of HeLa extract, and increasing concentrations (either 5, 25, or 100 nM) competitor Pu-triplexes as indicated above each lane. Competitors included the covalent triplex containing photocross-linked PODN 1 (lanes 3−5) and noncovalent triplexes containing 5′ deletions of the TFO ODN 1 Δ1-4 (lanes 6−8), Δ1-5 (lanes 9−11), and Δ1-7 (lanes 12−14). (A) HeLa NE. (B) HeLa S100.

included our standard cross-linked Pu-triplex containing the PODN 1 TFO, a Pu-triplex with an identical sequence but containing the diastereomeric phosphorothioate TFO OPS, a related Pu-triplex composed of the identical Pu-duplex and the GA-rich TFO ODN 2, and a Py-motif triplex (containing ODN 3). As shown in Figure 5, increasing concentrations of any Pu-triplex but not the Py-triplex competed with each of the shifted species, regardless of whether they contained NE or S100 proteins. Slight general differences in competition effectiveness between the different triplexes, with an order of effectiveness of OPS > PODN 1 > ODN 2, was noted. This trend is consistent with the propensity of these TFOs to form Pu-motif triplexes (*18*). As also seen in Figure 4, different shifted species had different propensities for being competed by Pu-triplex DNAs, with the order H3 > H2 > H4 > H1 generally being found. Notably, some specific differences were seen with different triplex competitors. For example, the OPS triplex was less able to inhibit formation of the NE H2 complex than the other phosphodiester-containing Pu-triplexes (Figure 5A, compare lane 4 or 10 and lane 7). Also, the Pu-triplex containing the GA-rich TFO ODN 2 was less able to inhibit formation of the H1 complex than either Pu-triplex containing GT-rich TFOs (compare lane 5 or 8 and lane 11). Taken together, these data indicate that these HeLa 3BPs specifically recognize Pu-motif triplexes, though not all types of Pu-triplexes were equally recognized by these proteins.

Previously we had shown through a survey of different TFOs and through combinatorial methods that the minimal length for optimal purine-motif triplex formation was 12−13 bt (*25*, *26*). If triplex formation potential was the primary criterion underlying Pu-triplex recognition by 3BPs, then maximal binding affinities would be found for these shorter triplexes. To test this hypothesis, binding reactions containing increasing concentrations (either 5, 25, or 100 nM) of unlabeled Pu-triplexes as competitor, either 19- (PODN 1), 15- (Δ1-4), 14- (Δ1-5), or 12-bt long (Δ1-7), were assembled and the products analyzed by EMSA. As shown in Figure 6, the 19-bt triplex was the most effective competitor, the 15- and 14-bt triplexes were intermediate in effectiveness,

and the 12-bt triplex was relatively ineffective in preventing binding of different 3BPs to the standard 19-bt Pu-triplex probe. Similar results were observed for both NE and S100 3BPs, and the individual sensitivity of different 3BPs to competition followed the trends observed previously (i.e., H3 most and H1 least). These findings indicated that, generally, 3BP-binding affinity increased with increasing Pu-triplex length. Additional studies will be necessary to determine whether this trend continues for even larger triplexes, suggestive of cooperative interactions between 3BPs, or whether an optimal 3BP binding site size exists.

Efficient assembly of purine-motif triplexes can be achieved by annealing a molar excess (typically 3−5-fold) of TFO to its duplex target in the presence of high Mg^{2+} concentrations (*18*). Obviously, under these conditions some free TFO remains in these triplex preparations. While data from our experiments with different labeled probes (Figure 3) demonstrated that 3BPs specifically recognized Pu-motif triplexes, they do not preclude the possibility that these proteins would also recognize other DNAs. To test this possibility, binding reactions were performed in the presence of increasing concentrations (50, 250, or 1000 nM) of different oligonucleotides. These included the CT-rich strand of the Pu-duplex target (Pu-CT), the GT-rich 19-mer TFO ODN 1, the GA-rich strand of the Pu-duplex target (Pu-GA), and the GA-rich 19-mer TFO ODN 2. EMSAs of binding reactions performed with these competitor DNAs, 1 nM labeled Pu-triplex, and either HeLa NE or S100 are shown in Figure 7. As seen there, the oligonucleotide Pu-CT was unable to inhibit formation of any of the 3BP complexes. ODN 1 was able to partially inhibit H3 complex formation, and to a lesser extent H2 and H4, when present at a 1000-fold molar excess compared to the labeled triplex probe (Figure 7A, lane 8). The Pu-GA oligonucleotide was more effective that ODN 1 in inhibiting formation of the H2 and H3 complexes (lane 11), though this was not a general characteristic of GA-rich oligonucleotides because comparable results were not seen with ODN 2 (lane 14). Similar competition assay results were observed with both NE and S100 3BPs. Together, these data indicate that the putative 3BPs could also recognize certain G-rich oligonucleotides, albeit with considerably lower affinity than for the 19-bt Pu-triplex. It should be noted that GT-rich oligonucleotides such as ODN 1 readily form intramolecular quadruplexes in the presence of K^+ (*27, 28*). Thus it is quite likely that these structures and not single-stranded DNA are the species actually being recognized by 3BPs.

Chromatography of HeLa 3BPs. Our evidence, including the differing representation of shifted species using either NE or S100 proteins (Figure 4) and the differential sensitivity of shifted species to various competitor DNAs (Figures 4, 5, and 7), supports our contention that several 3BPs exist in HeLa cells. Additional proof was sought through the analysis of chromatographic fractions derived from HeLa extracts. Chromatographic fractions investigated included the 0.1, 0.3, 0.5, and 1.0 M KCl eluates from a phosphocellulose (PC) cation-exchange column and the 0.1 and 0.3 M KCl eluates of a DEAE-cellulose (DE) anion-exchange column charged with the PC 0.5 step fraction (Figure 8A). Such fractions are equivalent to those commonly used to reconstitute class II gene transcription in vitro (*21*). These fractions were each incubated with the labeled Pu-triplex probe under conditions

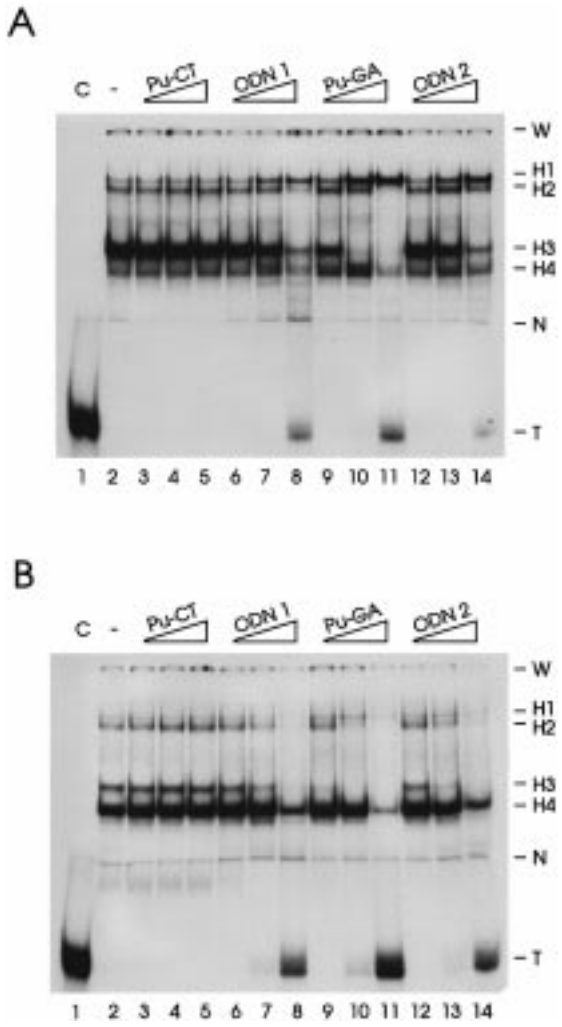

FIGURE 7: Competition of 3BP binding by oligonucleotides. EMSAs were performed on reaction mixtures containing 1 nM labeled Pu-triplex (PODN 1), 3 μg of HeLa extract, and increasing concentrations (either 50, 250, or 1000 nM) competitor oligonucleotides as indicated above each lane. Competitors included the CT strand of the Pu-duplex (lanes 3−5), the GT-rich TFO ODN 1 (lanes 6−8), the GA strand of the Pu-duplex (lanes 9−11), and the GA-rich TFO ODN 2 (lanes 12−14). (A) HeLa NE. (B) HeLa S100.

favoring 3BP binding, and the resulting complexes were analyzed by EMSA. As shown in Figure 8B, several shifted species were observed in the different chromatographic fractions. Complex H1 appeared enriched in the PC 0.1 fraction (compare lanes 2 and 3). Because no physical concentration of proteins occurs in a column breakthrough fraction, this apparent increase in affinity could reflect a relatively abundant 3BP that has a weaker affinity for Pu-triplexes than other 3BPs normally found in HeLa NE. The H2 complex was apparently not enriched in any of the chromatographic fractions, but a new shifted species (H3′) with a similar relative electrophoretic mobility ($R_f = 0.23$) appeared with the high-salt PC fractions coincident with the appearance of H3. Both the H3′ and H3 species were also present in the same DE fraction (DE 0.3); this co-chromatographic behavior is consistent with the presence of similar proteins in each complex. Evidence that these complexes contained 3BPs was obtained through competition experiments in which formation of both complexes was inhibited with a 100-fold molar excess triplex but not duplex DNA (lanes 8−10).

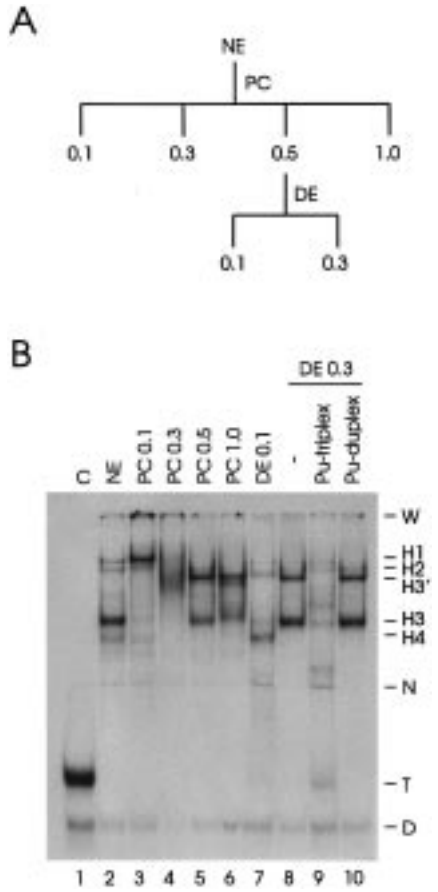

FIGURE 8: Chromatographic fractionation of 3BPs from HeLa NE. (A) Schematic representation of the chromatographic fractions investigated for 3BP activity. Molarities of the salt eluates used are indicated below. PC and DE refer to phosphocellulose and DEAE-cellulose matrixes, respectively. (B) EMSA of reaction mixtures containing 1 nM labeled Pu-triplex (PODN 1) and protein fractions as indicated. These included 3 μg of NE (lane 2), 10 μg of PC 0.1 (lane 3), 6 μg of PC 0.3 (lane 4), 4 μg of PC 0.5 (lane 5), 3 μg of PC 1.0 (lane 6), 1 μg of DE 0.1 (lane 7), and 2 μg of DE 0.3 (lanes 8−10). Reaction mixtures containing the DE 0.3 fraction also contained either no (lane 8), 100 nM Pu-triplex with PODN 1 (lane 9), or 100 nM Pu-duplex (lane 10) competitor DNA. A control reaction performed in the absence of added protein is also shown (C, lane 1).

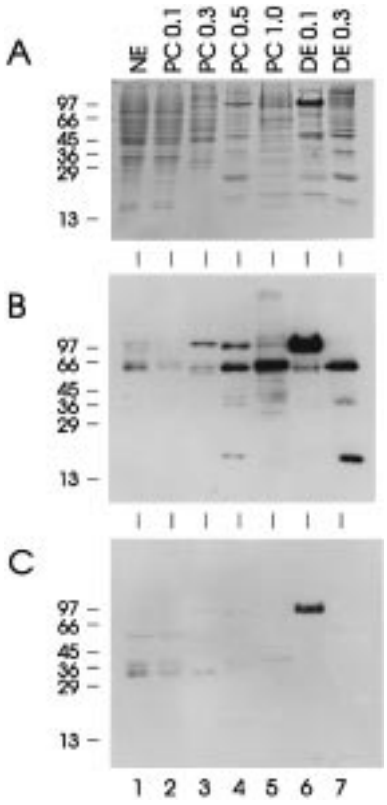

FIGURE 9: Identification of HeLa 3BPs. 3BPs present in chromatographic fractions derived from HeLa NE were resolved by SDS−PAGE and visualized by Southwestern blotting using either labeled Pu-triplex or Pu-duplex as a probe. Proteins fractions investigated included 7.5 μg each of NE (lane 1), PC 0.1 (lane 2), PC 0.3 (lane 3), PC 0.5 (lane 4), PC 1.0 (lane 5), DE 0.1 (lane 6), and DE 0.3 (lane 7). The relative mobilities and molecular weights of a series of marker proteins are indicated at left. (A) Coomassie-stained proteins. (B) Southwestern with Pu-triplex probe. (C) Southwestern with Pu-duplex probe.

Finally, the 3BP responsible for the H4 shift was predominantly found in the PC 0.5/DE 0.1 fraction (lane 7). Taken together, these data suggest that at least three 3BPs exist in HeLa cell extracts and that those responsible for the H1, H3, and H4 complexes possess sufficiently different chromatographic properties that they can be readily separated by simple ion-exchange chromatography.

Identification of HeLa 3BPs. While differences in competitor sensitivities and chromatographic behavior provide indirect evidence for the existence of different HeLa 3BPs, direct identification of the responsible proteins can be pursued by several methods. One of these is Southwestern blotting, in which proteins separated by SDS−PAGE are blotted onto nitrocellulose and probed with a radiolabeled DNA containing a desired sequence. To investigate the polypeptides responsible for specific Pu-triplex recognition, we electrophoresed and blotted proteins present in HeLa NE and the chromatographic fractions derived from NE described above and then probed this blot with a Pu-triplex probe containing photocross-linked PODN 1. Following exhaustive washing to remove nonspecifically bound probe, the polypeptides that continued to bind triplex probe were visualized by autoradiography. As shown in Figure 9B, several bands corresponding to proteins with molecular masses ranging from 15 to over 100 kDa were observed. More triplex probe was found associated with proteins present in the phosphocellulose step fractions (PC 0.3, 0.5, and 1.0) than in the NE or column breakthrough (PC 0.1) fractions. This is understandable given the protein concentration, typically on the order of 10-fold, that occurs following phosphocellulose chromatography (*21*). Major bands included a 100-kDa species present in the PC 0.3, 0.5, and DE 0.1 fractions, a 60-kDa species present in the PC 0.5, 1.0, and DE 0.3 step fractions, and a 15-kDa species present in the PC 0.5 and DE 0.3 fractions. Several other minor species were also noted.

To confirm the Pu-triplex binding specificity of these interactions, Southwestern blotting using the corresponding Pu-duplex probe was performed. As shown in Figure 9C, while several proteins showed stronger binding to the duplex probe than to the triplex probe (e.g., those in the 30−45 kDa range present in NE and the PC 0.1 fraction; compare Figures 9B and 9C, lanes 1 and 2), those species demonstrating the strongest triplex binding all showed appreciably weaker binding to duplex DNA. Significant duplex binding was still observed with the 100-kDa protein, which also happened to

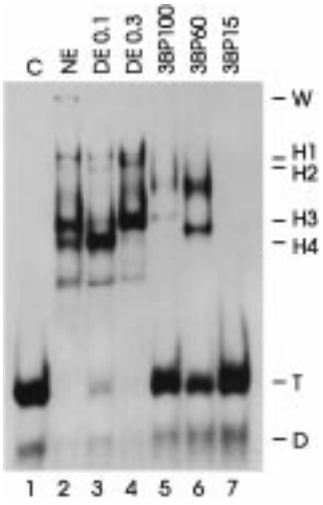

FIGURE 10: Identification of proteins responsible for 3BP-triplex complexes. Extracts from acrylamide slices containing either the 100-, 60-, or 15-kDa species identified by Southwestern blotting were incorporated into standard triplex binding reactions containing radiolabeled Pu-triplex probe and the resulting complexes resolved by EMSA. Controls included the free probe alone (C, lane 1) or together with 0.8 μg of NE (lane 2), 0.2 μg of DE 0.1 (lane 3), or 0.5 μg of DE 0.3 (lane 4) chromatographic fractions. Relative mobilities of the previously described 3BP−triplex complexes are indicated at right.

be a major protein species in the DE 0.1 fraction (Figure 9A). Given the large amount of this protein present and its chromatographic properties (i.e., high-affinity binding to a cation exchanger and no binding to an anion exchanger), it is likely its recognition of both triplex and duplex probes actually reflects a weak electrostatic interaction between an abundant positively charged protein and the negatively charged DNA probes. Here the apparent specificity might result from the increased negative charge density inherent to triple-helical DNA and may not reflect a true specific recognition of the Pu-motif triplex.

Correspondence between 3BPs Identified by EMSAs and Southwestern Blots. EMSAs and Southwestern blots are significantly different methods for studying DNA-binding proteins. The former identifies protein−DNA complexes that survive native gel electrophoresis, while the latter identifies proteins that preferentially bind a DNA probe following SDS−PAGE and blotting onto a nitrocellulose membrane. To bring together the data obtained by both methods, we sought to determine whether there was a direct correspondence between the proteins identified by Southwestern blots and the proteins responsible for the complexes identified by EMSA. An SDS−PAGE was performed essentially as described in Figure 9. Prior to Coomassie staining, regions of the gel corresponding to the 90−110 kDa range for the DE 0.1 fraction and the 50−60 and 14−18 kDa ranges for the DE 0.3 fraction were excised and incubated at 4 °C overnight in an equal volume of 20 mM Tris-HCl (pH 7.3), 100 mM KCl, 0.2 mM EDTA, 0.05% Triton X-100, and 1 mM dithiothreitol. Standard triplex binding reactions were then performed, and the products were analyzed by EMSA. As shown in Figure 10, a reaction containing the 100-kDa species demonstrated two faint bands with R_f's of 0.28 and 0.39 (lane 5). Likewise, the 60 kDa-containing reaction demonstrated two bands with R_f's of 0.29 and 0.40 (lane 6). No shifted species was observed with the 15-kDa species (lane 7). Note that the faster mobility shift observed with the 60-kDa species was similar to the major shifted species, H3, observed with its parent DE 0.3 fraction (compare lanes 4 and 6). Similar correlations were not found with the other species. Although this can be interpreted as indicating that the proteins identified by Southwestern blotting do not correspond to those present in the major complexes identified by EMSA, it is also possible that previously denatured proteins do not always yield identical electrophoretic mobility protein−triplex complexes as their native counterparts, thus complicating their analysis.

DISCUSSION

Using a well-defined purine-motif triplex as part of an investigation by EMSA and Southwestern methods, we identified several human proteins that specifically recognized triple-helical DNA. These proteins were present in both nuclear and cytoplasmic extracts, though their distributions in each differed. Competition experiments demonstrated that these proteins preferentially bound G-rich purine-motif triplexes, with the longer triplexes exhibiting greater affinity. Structural elements such as the presence of T*AT versus A*AT base triplets or a phosphodiester versus phosphorothioate third strand had little effect on binding affinity. A weak affinity was also noted for G-rich oligonucleotides. Chromatographic and Southwestern data suggest that there were at least three different proteins responsible for these binding activities.

This is the first report of triplex-binding proteins that specifically recognize Pu-motif DNA. Two laboratories have described human proteins that recognize Py-motif triple helixes (*15*, *16*). Kiyama and Camerini-Otero described a set of 55-kDa human proteins that bound to a $(dT)_{34}\cdot(dA)_{34}\cdot(dT)_{34}$ triplex oligonucleotide. Substantial affinity was also observed for these proteins and the duplex oligonucleotide $(dA)_{34}\cdot(dT)_{34}$. Guieysse et al. described a 55-kDa human protein that bound a hairpin oligonucleotide containing the target duplex (5′-dAAAAGGAGAGGGAGA-3′)·(5′-dTCTC-CCTCTCCTTTT-3′) and the triplex-forming sequence (5′-dZZZZCCZCZCCCZCT-3′), where Z corresponds to the base bromodeoxyuridine. Some affinity could also be observed with hairpins that do not form stable triplexes, two target duplexes separated by an oligo dT linker, a purine-motif triplex based on this duplex target, and a $(dT)_{34}$ oligonucleotide. None of these proteins is likely to be one of those investigated by our laboratory. However, this possibility cannot be completely excluded until their corresponding cDNAs have been cloned. In fact, experiments using the photocross-linked Py-triplex containing PODN 3 demonstrated multiple novel shifted species, though these did not correspond to those found with Pu-triplexes (M. Musso, unpublished observations). Rather, it is more likely that different proteins recognize the different triplex motifs, with different triplex sequences being preferentially bound by certain 3BPs.

Identical 3BPs, though in different proportions, were found in HeLa nuclear and cytoplasmic extracts. While it is difficult to conceive of a role for triplex-binding proteins outside of the nucleus, possible substrates might include mitochondrial DNA or the highly structured RNAs present in the ribosome. Another possibility is that all 3BPs are

actually nuclear in location, with some partitioning into the cytoplasmic fraction as a result of the extraction procedure. Such is reminiscent of the proteins involved in class III gene transcription, many of which are quite abundant in the HeLa S100 (*29*). Alternatively, certain 3BPs could reside in a cytoplasmic compartment, potentially in a latent form, to be later activated and translocated into the nucleus only when so required. In this case transcription factors such as NF-κB provide a useful paradigm (*30*). Once antibodies are available against 3BPs, immunofluorescence microscopy should allow the determination their true cellular localizations. Ultimately this information could provide clues as to the biological roles of these proteins.

Our competition data provide some information on the possible Pu-motif structural elements recognized by Pu-3BPs. The ODN 1-based triplex investigated here was characterized by four sets of three or four adjacent G*GC base triplets punctuated by T*AT base triplets. Substituting A*AT base triplets for T*AT only slightly reduced the affinity for most of the HeLa 3BPs, which could be explained by the reduced ability of GA-rich compared to GT-rich TFOs to form purine-motif triplexes (*3, 18, 22*). Likewise, substituting a diastereomeric phosphorothioate backbone for the normal phosphodiester backbone on the triplex third strand had little effect on the binding affinity of these proteins. Note that both of these structural alterations involved changes within the original major groove of the parent duplex. Thus it is interesting to speculate that Pu-3BPs primarily recognize a triplex through its duplex face, potentially involving interactions in what was the duplex minor groove. Additional studies with modified duplexes should be able to answer this question.

We found that certain Pu-3BPs had a weak affinity for G-rich oligonucleotides. It should be noted that under the experimental conditions used (i.e., 50 mM K^+), these oligonucleotides have been found to exist not as single-stranded DNAs but primarily as inter- or intramolecular quadruplexes (*27, 28*). Quadruplexes are characterized by stacks of two or more square planar arrays of four guanines, where each is a donor and acceptor of two Hoogsteen hydrogen bonds. Thus they offer similar high negative charge densities and Hoogsteen hydrogen bonding as found in G-rich Pu-motif triplexes. Proteins have been identified in yeast, *Tetrahymena thermophila*, and mammalian cells that recognize quadruplex DNAs (reviewed in 31). Of these, those found in rabbit and rat hepatocytes, including the 57-kDa QUAD protein (*32*), qTBP42 (*33*), and uqTBP25 (*34*), are most likely the closest homologues of human quadruplex binding proteins. On the basis of several lines of evidence, including their apparent molecular masses, limited heat stability, and very low affinity for intra- and intermolecular G/T-rich quadruplex DNAs, we do not believe our Pu-3BPs correspond to any of these quadruplex-binding proteins (L. Nelson, unpublished observations). However, this does not preclude the possibility that Pu-3BPs can also recognize other DNA sequences or structures that we have yet to investigate, much as the murine quadruplex-binding protein qTBP42 has been found to also avidly bind duplex DNA containing the CArG box motif, 5′-CC$(A/T)_6$GG-3′ (*35*).

Differences in competition efficiencies for the different shifted species suggested that multiple Pu-3BPs were present in HeLa extracts. This was borne out by simple chromatographic fractionation of HeLa nuclear extracts, where passage through two ion exchangers was sufficient to separate the proteins responsible for the H1, H3, and H4 shifts. Southwestern blotting methods also indicated several protein species capable of specifically recognizing Pu-triplex DNA. It is tempting to make a simple correspondence between the proteins identified by Southwestern blotting and the shifts present in the chromatographic fractions; however, such could not be done with our data. Likewise, attempts to identify the molecular masses of the protein present in the different EMSA bands using Southwestern methods have yet to prove successful (L. Nelson, unpublished observations). The reciprocal experiment, identifying the EMSA shifts resulting from a particular protein, was able to show Pu-triplex complexes for two of the proteins identified by Southwestern methods. Yet only in one case did a renatured 3BP-triplex complex demonstrate a similar electrophoretic mobility as a native 3BP-triplex complex (that being for the 60-kDa 3BP and the H3 complex). It should be realized that Southwestern methods require that the protein domains responsible for specific DNA binding be efficiently and effectively renatured and that the polypeptides required for forming an active protein have nearly identical molecular weights. Thus, the full complement of proteins responsible for each shifted species may not be identified by this method. Alternatively, proteins that might not normally interact with a specific DNA may appear to do so by Southwestern methods, especially if it is very abundant and there is a weak, nonspecific affinity. Further purification of these proteins, ideally to homogeneity, cloning of their cDNAs, and expression of recombinant proteins will ultimately allow a more complete definition of 3BPs.

HeLa cell extracts were found to contain proteins that specifically bind triplex DNA. However, this finding does not prove that the cellular functions of these proteins is to interact with triplexes, nor that even triple-helical DNA exists in vivo. Similar 3BPs have been identified in a yeast whole cell extract (M. Musso, manuscript in preparation), suggesting conserved roles for these proteins in all eukaryotes. This observation of 3BPs in yeast also opens the possibilities of relatively easy cloning of their respective genes and powerful genetic analyses of their cellular functions. Ultimately, these studies should yield answers as to the biological roles of triple-helical DNAs and the proteins that bind them.

Oligonucleotides that form triple helixes have been promoted as possible gene therapeutics (*36, 37*). This "antigene" approach, typically requires triplex formation at a specific site within a gene promoter/enhancer region, whereby this triplex interferes with required *trans*-activating protein binding, resulting in decreased targeted gene expression. While some evidence for the feasibility of this approach exists, the ramifications of cellular 3BPs in this phenomenon have yet to be considered. Triplex-binding proteins could stabilize triplexes that would otherwise be unstable under physiological conditions, thereby facilitating an antigene effect. Alternatively, a particular bound 3BP could itself affect transcription, either positively or negatively. Potentially, a 3BP could even signal a cellular process (e.g., recombination or repair) that would affect a template DNA directly. Finally, binding of 3BPs to synthetic triplexes may deplete available pools of these proteins, thereby globally interfering with normal cellular functions. Triplex

DNA offers a possible means for targeting specific DNA sequence within an entire genome. Understanding of the biochemistry and biological roles of 3BPs will allow us to better predict the consequences of such actions.

ACKNOWLEDGMENT

We thank Michèle Sawadogo for critical reading of this manuscript.

REFERENCES

1. Felsenfeld, G., Davies, D. R., and Rich, A. (1957) *J. Am. Chem. Soc. 79*, 2023−2024.
2. Frank-Kamenetskii, M. D., and Mirkin, S. M. (1995) *Annu. Rev. Biochem. 64*, 65−95.
3. Beal, P. A., and Dervan, P. B. (1992) *Nucleic Acids Res. 20*, 2773−2776.
4. Greenberg, W. A., and Dervan, P. B. (1995) *J. Am. Chem. Soc. 117*, 5016−5022.
5. Lyamichev, V. I., Mirkin, S. M., and Frank-Kamenetskii, M. D. (1985) *J. Biomolec. Struct. Dyn. 3*, 327−338.
6. Mirkin, S. M., and Frank-Kamenetskii, M. D. (1994) *Annu. Rev. Biophys. Biomol. Struct. 23*, 541−576.
7. Agazie, Y. M., Burkholder, G. D., and Lee, J. S. (1996) *Biochem. J. 316*, 461−466.
8. Kohwi, Y., and Kohwi-Sigamatsu, T. (1991) *Genes Dev. 5*, 2547−2554.
9. Baran, N., Lapidot, A., and Manor, H. (1987) *Mol. Cell. Biol. 7*, 2636−2640.
10. Rooney, S., and Moore, P. D. (1995) *Proc. Natl. Acad. Sci. U.S.A.* 92, 2141−2144.
11. Kolluri, R., Torrey, T. A., and Kinniburgh, A. J. (1992) *Nucleic Acids Res. 20*, 111−116.
12. Muraiso, T., Nomoto, S., Yamazaki, H., Mishima, Y., and Kominari, R. (1992) *Nucleic Acids Res. 20*, 6631−6635.
13. Hollingsworth, M. A., Closken, C., Harris, A., McDonald, C. D., Pahwa, G. S., and Maher, L. J. (1994) *Nucleic Acids Res. 22*, 1138−1146.
14. Horowitz, E. M., Maloney, K. A., and Ley, T. J. (1994) *J. Biol. Chem. 269*, 14130−14139.
15. Kiyama, R., and Camerini-Otero, R. D. (1991) *Proc. Natl. Acad. Sci. U.S.A. 88*, 10450−10454.
16. Guieysse, A. L., Praseuth, D., and Hélène, C. (1997) *J. Mol. Biol. 267*, 289−298.
17. Sawadogo, M., and Van Dyke, M. W. (1991) *Nucleic Acids Res. 19*, 674.
18. Musso, M., and Van Dyke, M. W. (1995) *Nucleic Acids Res. 23*, 2320−2327.
19. Musso, M., Wang, J. C., and Van Dyke, M. W. (1996) *Nucleic Acids Res. 24*, 4924−4932.
20. Abmayr, S. M., and Workman, J. L. (1988) in *Current Protocols in Molecular Biology* (Ausubel, F. M., Brent, R., Kingston, R. E., Moore, D. D., Seidman, J. G., Smith, J. A., and Struhl, K., Eds.) pp 12.1.1−12.1.9, Wiley-Interscience: New York.
21. Sawadogo, M., and Roeder, R. G. (1985) *Proc. Natl. Acad. Sci. U.S.A. 82*, 4394−4398.
22. Beal, P. A., and Dervan, P. B. (1991) *Science 251*, 1360−1363.
23. Hacia, J. G., Wold, B. J., and Dervan, P. B. (1994) *Biochemistry 33*, 5367−5369.
24. Cheng, A. J., and Van Dyke, M. W. (1993) *Nucleic Acids Res. 21*, 5630−5635.
25. Cheng, A. J., and Van Dyke, M. W. (1994) *Nucleic Acids Res. 22*, 4742−4747.
26. Hardenbol, P., and Van Dyke, M. W. (1996) *Proc. Natl. Acad. Sci. U.S.A. 93*, 2811−2816.
27. Guschlbauer, W., Chantot, J. F., and Thiele, D. (1990) *J. Biomol. Struct. Dyn. 8*, 491−511.
28. Cheng, A. J., and Van Dyke, M. W. (1997) *Gene 197*, 253−260.
29. Van Dyke, M. W., and Roeder, R. G. (1987) *Nucleic Acids Res. 15*, 5031−5039.
30. Baeuerle, P. A., and Baltimore, D. (1988) *Cell 53*, 211−217.
31. Rhodes, D., and Giraldo, R. (1995) *Curr. Opin. Struct. Biol. 5*, 311−322.
32. Weisman-Shomer, P., and Fry, M. (1993) *J. Biol. Chem. 268*, 3306−3312.
33. Sarig, G., Weisman-Shomer, P., Erlitzki, R., and Fry, M. (1997) *J. Biol. Chem. 272*, 4474−4482.
34. Erlitzki, R., and Fry, M. (1997) *J. Biol. Chem. 272*, 15881−15890.
35. Sarig, G., Weisman-Shomer, P., and Fry, M. (1997) *Biochem. Biophys. Res. Commun. 237*, 617−623.
36. Hélène, C. (1991) *Anti-Cancer Drug Des. 6*, 569−584.
37. Maher, L. J. (1992) *BioEssays 14*, 807−815.

BI9717486